JOURNAL OF MATERIALS SCIENCE 20 (1985) 2335–2344

Thermal and dielectric properties of rare earth iodates

B. P. GHOSH, K. NAG*
Department of Inorganic Chemistry, Indian Association for the Cultivation of Science, Calcutta 700 032, India

The thermal (TGA, DTA and DSC) and dielectric behaviour of all rare earth iodates (except prometheum) has been investigated. The iodates of lanthanum, cerium to europium and gadolinium to lutetium decompose differently and the activation energies for these decomposition reactions have been determined. The DSC measurements have shown that all of the anhydrous iodates undergo one or more exothermic/endothermic changes. From the nature of the DSC profiles, heat of transitions, and powder diffraction data the phase transformations of Ln $(IO_3)_3$ have been found to occur in four different ways (lanthanum, cerium to europium, gadolinium to terbium, dysprosium to lutetium). Dielectric measurements of Ln $(IO_3)_3$ at varying temperature have corroborated the observations made with DSC studies. Relatively low dielectric constants of the high-temperature phases probably indicate their centrosymmetric structures. The dielectric behaviour of noncentrosymmetric Ln $(IO_3)_3 \cdot H_2O$ (Ln = cerium to samarium) has been investigated in the temperature range 30 to $-160°$ C. They have high dielectric constants (ϵ_r, ~ 1800 to 2400) at the ambient temperature and do not show significant change in the entire temperature range of investigation.

1. Introduction

Solid state properties of rare earth iodates have been the subject of considerable studies [1–8] during recent years. The stimulus for such investigations was received from the fact that α-iodic acid and some of its salts show piezoelectric and pyroelectric properties [9–11].

A survey of crystallographic and nonlinear optical properties of various hydrated and anhydrous rare earth iodates has revealed [3] that they may be classified into thirteen crystallographic groups. Among the six anhydrous varieties (designated as types I to VI), only for type I (Ln = cerium to lutetium) and II (Ln = ytterbium, lutetium) have the space groups been determined (both centrosymmetric, but different); in the remaining cases (type III: Ln = cerium to samarium; type IV: Ln = lanthanum to praseodymium; type V: Ln = cerium to samarium; type VI: Ln = lanthanum) classification has been made on the basis of their powder diffraction data. Among the hydrates, the most interesting compounds are Ln $(IO_3)_3 \cdot 0.5H_2O$ (Ln = lanthanum) and Ln $(IO_3)_3 \cdot H_2O$ (Ln = cerium to samarium), both have noncentrosymmetric space groups and generate second harmonies more efficiently than quartz [3]. X-ray crystal structures have been determined for $Nd(IO_3)_3 \cdot H_2O$ [4], $Gd(IO_3)_3$ [5], $Pr(IO_3)_3 \cdot HIO_3$ [8] and $3La(IO_3)_3 \cdot HIO_3 \cdot 7H_2O$ [8]. For $Nd(IO_3)_3 \cdot H_2O$ piezoelectric and pyroelectric properties have been studied [7].

The thermal behaviour (TGA and DTA) of rare earth iodates as investigated by different workers [1, 2, 12–14] has shown significant differences. These differences are reflected both in the nature of the phase transitions of anhydrous iodates and their decomposition patterns.

The purpose of the present study has been three-fold. First, to investigate thermal stabilities of rare earth iodates particularly with a view to

*To whom correspondence should be addressed.

0022–2461/85 $03.00 + .12

ascertaining the nature of decomposition reactions from nonisothermal kinetic measurements. Second, to study the phase transitions of anhydrous iodates from differential scanning calorimetric (DSC) measurements. Finally, to investigate the dielectric properties of anhydrous iodates as a function of temperature and frequency and to see how they correlate with the observations made from DSC measurements. The dielectric properties of noncentrosymmetric hydrates have also been of interest to us. The thermal and dielectric properties of $La(IO_3)_3 \cdot 0.5H_2O$ and $La(IO_3)_3$ have been previously reported by us [15, 16].

2. Experimental procedure

2.1. Preparation of rare earth iodates

2.1.1. $Ln(IO_3)_3 \cdot xH_2O$ (Ln = lanthanum to lutetium; $2 \leqslant x \leqslant 4$)

Rare earth oxides 99.9% pure (Koch-Light) were converted to their neutral nitrates and used for preparation. To an aqueous solution (500 cm^3) of $Ln(NO_3)_3 \cdot 6H_2O$ (5 mmol) an aqueous solution (100 cm^3) of potassium iodate (16 mmol) was added and stirred at the ambient temperature. The mixture was additionally stirred for 15 min. The precipitate that formed was collected by filtration, washed freely with water, and dried over $CaCl_2$ for several days.

2.1.2. $Ln(IO_3)_3 \cdot H_2O$ (Ln = cerium, praseodymium, neodymium, samarium)

The precipitation was carried out in the same way as described above by mixing the two solutions at their boiling temperature [2]. The mixture was boiled further for 15 min, filtered hot, and the residue was washed with boiling water. The compound was finally dried over $CaCl_2$.

2.1.3. $La(IO_3)_3 \cdot 0.5H_2O$

The method of preparation is the same as $Ln(IO_3)_3 \cdot H_2O$. Anhydrous rare earth iodates used for dielectric measurements were obtained by heating $Ln(IO_3)_3 \cdot xH_2O$ at 320 ± 10° C to a constant weight.

2.2. Thermal analysis

Thermogravimetric and differential thermal analyses (TGA and DTA) were carried out in a Shmadzu DT-30 thermal analysis system by heating the samples (15° C min^{-1}) in an atmosphere of nitrogen up to 1000° C.

Differential scanning calorimetric (DSC) measurements were performed on a Perkin–Elmer DSC-2 equipment in the temperature range 350–900 K, under a constant flow rate of nitrogen. The sample was contained in an aluminium pan and lid assembly by crimping. A matched gold pan served as the reference material. For the purpose of determining enthalpy changes during phase transitions several calibration curves were drawn with high-purity indium, zinc and tin of accurately-known heats of fusion [17].

2.3. Dielectric measurements

The relative dielectric constant, ϵ_r, of a material was determined as the ratio $\epsilon_r = \epsilon/\epsilon_0 = C/C_0$ where C is the capacitance of a parallel plate condenser containing the sample, C_0 is the corresponding capacitance for the empty space in vacuum. The capacitance and dielectric loss ($\tan \delta$) measurements were carried out with a Radart-1204, 0.1% LCR bridge (India) in conjunction with a Radart-926 audio oscillator operating in the frequency range 15 Hz to 50 kHz.

The specimens were pelletized by subjecting them to a pressure of 5 kbar (5×10^5 Nm^{-2}) for 5 to 10 min. The diameter of the pellets was 13.5 mm and the thickness varied from 1 to 2 mm. A very thin layer of silver (for subambient measurements) or palladium (for higher temperature work) paste (Dow-Corning) was applied to both surfaces of the pellet in order to obtain good contact with the metal electrodes. For capacitance measurements a spring-loaded locally fabricated two-terminal sample holder was used. The sample holder contained two circular probes made of polished stainless steel having a 1.4 cm diameter. The sample holder with properly insulated connecting leads was fitted in a stainless steel cylinder that could be evacuated to 10^{-5} to 10^{-6} torr. A thermocouple (chromel/alumel or copper/constantan) was placed close to the specimen and the potential drop was measured with a Leeds-Northup-type K-4 potentiometer. For measurements above the ambient temperature a cylindrical furnace in combination with a temperature controller was used for heating. For measurements at subambient temperatures a locally fabricated cryogenic autocooling device was used [18].

X-ray powder patterns were obtained with a Debye–Scherrer or Guinnier camera using Cu$K\alpha$ radiation.

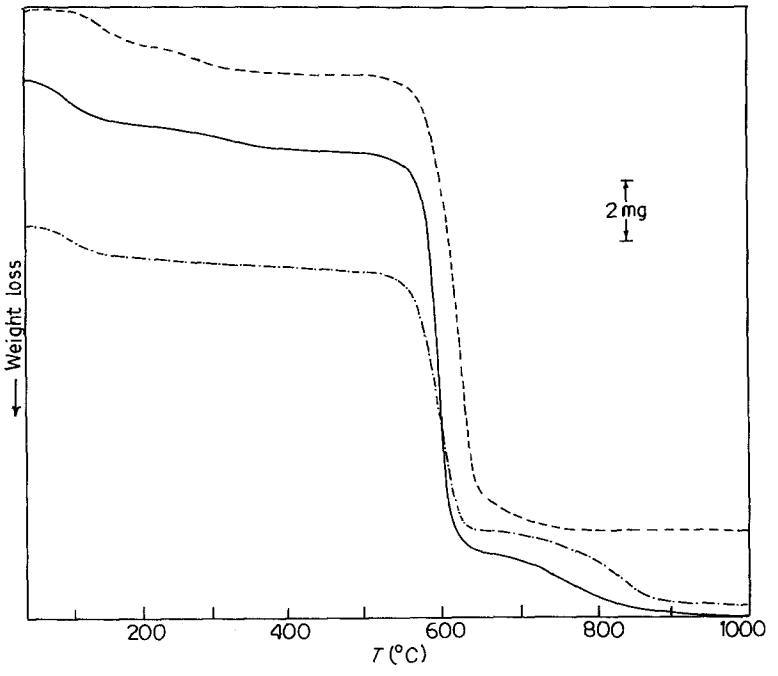

Figure 1 Thermogravimetric analysis of hydrated rare earth iodates. $La(IO_3)_3 \cdot 3.5H_2O$ (– · – · – 15.8 mg); $Nd(IO_3)_3 \cdot 3.5H_2O$ (——— 22.7 mg); $Tm(IO_3)_3 \cdot 4H_2O$ (– – – 23 mg).

3. Results and discussion

3.1. Thermal analysis

The rare earth iodates prepared at ambient temperature have the composition $Ln(IO_3)_3 \cdot xH_2O$ ($2 \leqslant x \leqslant 4$)*. The number of water molecules present and the purity of the products were determined from TGA. All of them begin to lose water molecules as low as 50° C, yet complete dehydration occurs at 250 to 300° C (see Fig. 1). From the nature of DTA (not shown in Fig. 1) it appears that at least one water molecule is coordinately bound with the metal ions. The compositions $La(IO_3)_3 \cdot 0.5H_2O$ and $Ln(IO_3)_3 \cdot H_2O$ have also been confirmed from thermal analysis. No powder diffraction pattern could be obtained for the compounds $Ln(IO_3)_3 \cdot xH_2O$ ($2 \leqslant x \leqslant 4$; Ln = lanthanum to terbium) showing that all of them are amorphous. The diffraction patterns for $Ln(IO_3)_3 \cdot 4H_2O$ (Ln = dysprosium to lutetium) are all similar and agree well with those reported in the literature [3]. Similarly the observed *d*-spacings of $La(IO_3)_3 \cdot 0.5H_2O$ and $Ln(IO_3)_3 \cdot H_2O$ are in agreement with the reported values [3].

The anhydrous iodates undergo several phase transitions in the temperature range 350 to 500° C (see later). They begin to decompose between 500 and 540° C. As stated earlier, there is considerable disagreement among various authors [1, 2, 12–14] regarding the products of decomposition. In the case of $La(IO_3)_3$, the following decomposition reactions take place (Fig. 1):

$$10La(IO_3)_3 \longrightarrow 2La_5(IO_6)_3 + 12I_2 + 27O_2$$

$$4La_5(IO_6)_3 \longrightarrow 10La_2O_3 + 6I_2 + 21O_2 \quad (1)$$

The weight losses observed for the iodates of Ln = praseodymium, neodymium, samarium, europium, are in agreement with the decomposition reaction

$$7Ln(IO_3)_3 \longrightarrow Ln_5(IO_6)_3 + Ln_2O_3 + 9I_2 + 21O_2 \quad (2)$$

The intermediate product $Ln_5(IO_6)_3 \cdot Ln_2O_3$ decomposes to the oxide in the next step (Fig. 1). In the case of cerium, CeO_2 is the final decomposition product. The higher lanthanides (Ln = gadolinium to lutetium) all decompose to the corresponding oxide in a single step (Fig. 1):

$$4Ln(IO_3)_3 \longrightarrow 2Ln_2O_3 + 6I_2 + 15O_2 \quad (3)$$

Table I summarizes the observed and calculated weight losses for the decomposition Reactions 1 to 3. It may be pointed out that unlike a previous report [12], no correlation between the temperature for onset of decomposition and the atomic number of the lanthanide has been observed.

*Terbium: $2H_2O$; cerium, samarium, europium, gadolinium: $3H_2O$; lanthanum, praseodymium, neodymium: $3.5H_2O$; dysprosium to lutetium: $4H_2O$.

TABLE I Observed and calculated weight losses for the decomposition Reactions 1 to 3 and corresponding activation energies, E_a^*

$Ln(IO_3)_3$	Weight loss (%)*	Decomposition reaction	E_a^* (kcal mol^{-1})
La	59.4 (59)	1	92†, 86‡
Pr	63 (63.4)	2	70†, 74‡
Nd	62.5 (63.1)	2	75†, 69‡
Sm	63 (62.6)	2	68†, 72‡
Gd	74 (73.4)	3	
Dy	73 (72.8)	3	
Tm	71.6 (72.2)	3	84†, 80‡
Yb	72.1 (71.7)	3	

*Calculated values are in parentheses.
†Method due to Horowitz and Metzger [19].
‡Method due to Coats and Redfern [20].

3.2. Kinetics of thermal decomposition

Nonisothermal decomposition kinetics for the rare earth iodates were determined from the TGA curves. Two commonly used methods, namely those of Horowitz and Metzger [19] and Coats and Redfern [20], were used for evaluation of the activation energies, E_a^*. Previous work in this laboratory [21, 22] showed that these two methods afford consistent results. The activation energies obtained for several rare earth elements are shown in Table I. Noticeable differences in the activation energy parameters for $Ln(IO_3)_3$ (Ln = praseodymium, neodymium, samarium) with La $(IO_3)_3$ and $Tm(IO_3)_3$ again support the occurrence of three different types of decomposition reactions.

3.3. DSC measurements of anhydrous $Ln(IO_3)_3$

The DTA of anhydrous iodates shows the presence of one or more exotherm/endotherm in the temperature range 350 to 500° C. For more detailed information DSC studies were carried out. The materials used for DSC measurements were obtained by dehydrating the hydrated compounds in the Shimadzu DT-30 TGA/DTA system at the appropriate temperatures. All of the anhydrous materials used were found from X-ray diffraction studies to be amorphous.

The behaviour of $La(IO_3)_3$ has been reported previously [15, 16]. This compound is characterized by the presence of two overlapping exotherms at 357 and 362° C and an endotherm at 493° C.

The nature of the phase transitions in the iodates of cerium, praseodymium, neodymium, samarium and europium are similar. The DSC profiles of $Pr(IO_3)_3$ and $Nd(IO_3)_3$ are shown in Fig. 2. All of these compounds undergo three consecutive exothermic changes in the temperature range 340 to 460° C. In the cases of samarium and europium the first two peaks are not clearly resolvable. X-ray powder data for the quench-cooled specimens of $Nd(IO_3)_3$ at 370, 400 and 460° C were found to correspond with the types V, IV and I, respectively.

Fig. 3 shows the thermal behaviour of $Gd(IO_3)_3$ and $Dy(IO_3)_3$. In both cases a single exothermic change occur. The phase isolated at 420° C for $Gd(IO_3)_3$ corresponds to the type I species.

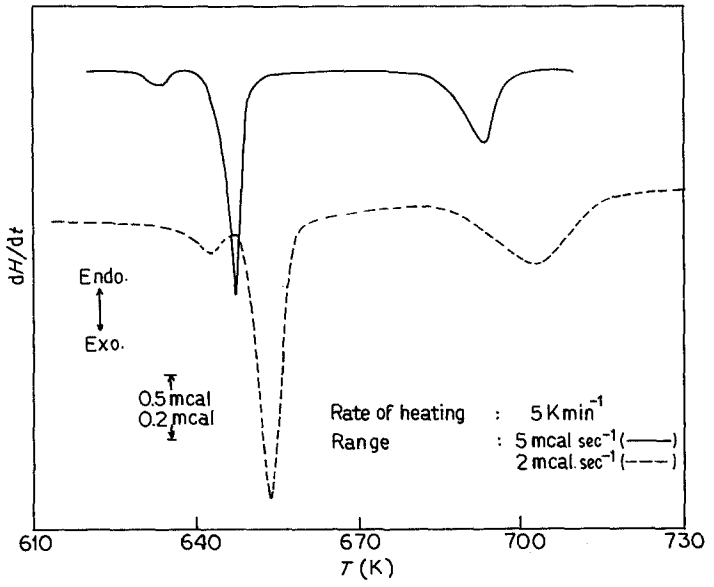

Figure 2 DSC thermograms of Pr $(IO_3)_3$ (——) and $Nd(IO_3)_3$ (– – –).

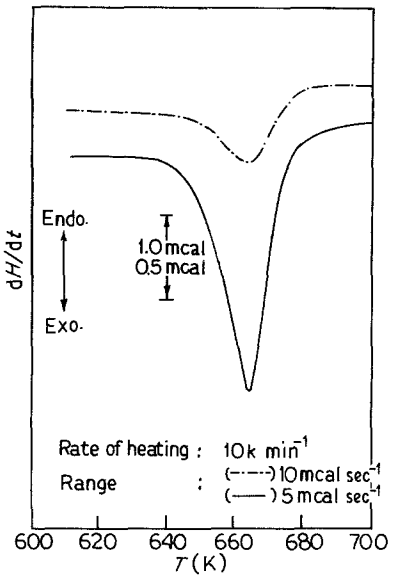

Figure 3 DSC thermograms of $Gd(IO_3)_3$ (———) and $Tb(IO_3)_3$ (–·–·–).

The DSC thermograms of the remaining six iodates (dysprosium to lutetium) have similar features, namely a weak endothermic change at about 375° C followed by a very strong exothermic process at about 390° C. The behaviour of dysprosium, holmium and erbium iodates are shown in Fig. 4. No powder data were obtained before and after the endothermic effect, the phase obtained after the exothermic change corresponds to the type I iodates.

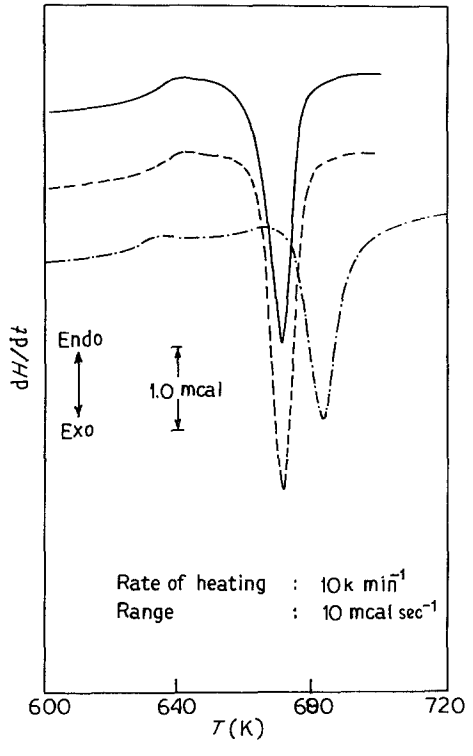

Figure 4 DSC thermograms of $Dy(IO_3)_3$ (———); $Ho(IO_3)_3$ (— — —); $Er(IO_3)_3$ (–·–·–).

TABLE II Phase transition temperatures (T_m) and enthalpy changes (ΔH) obtained from DSC measurements

$Ln(IO_3)_3$	T_m^*(° C)	Nature of transition	ΔH(kcal mol^{-1})
La	357, 362	Am → ? → Am	5
	493	IV → VI	2.5
Ce	347	Am → V	0.3
	360	V → IV	3.9
	398	IV → I	0.5
Pr	360	Am → V	0.4
	375	V → IV	4.1
	420	IV → I	2.0
Nd	369	Am → V	0.4
	381	V → IV	4.2.
	430	IV → VI	2.2
Sm	370	Am → V	
	392	V → IV	4.4
	444	IV → I	2.4
Eu	372	Am → V	
	392	V → IV	4.5
	440	IV → I	2.8
Gd	391	Am → I	2.5
Tb	390	Am → I	2.3
Dy	366	Am → Am	
	398	Am → I	9.2
Ho	368	Am → Am	
	399	Am → I	9.6
Er	362	Am → Am	
	410	Am → I	10.8
Tm	362	Am → Am	
	399	Am → I	10.4
Yb	382	Am → Am	
	409	Am → I	10.5
Lu	367	Am → Am	
	392	Am → I	10.5

*Peak tempeatures of DSC curves.
Am stands for amorphous; the Roman numericals indicate the type of anhydrous iodate.

Table II summarizes the peak temperatures (T_m) for phase transformations and the corresponding enthalpy changes for all anhydrous iodates. The classification made on the basis of the DSC profiles (lanthanum; cerium to europium; gadolinium, terbium; dysprosium to lutetium) is also consistent with the ΔH values of the compounds. It may be further noted that the decomposition patterns for these compounds are in harmony with the observations made here. A unique feature in the chemistry of rare earth elements is their close resemblance to each other in chemical and physical properties as a consequence

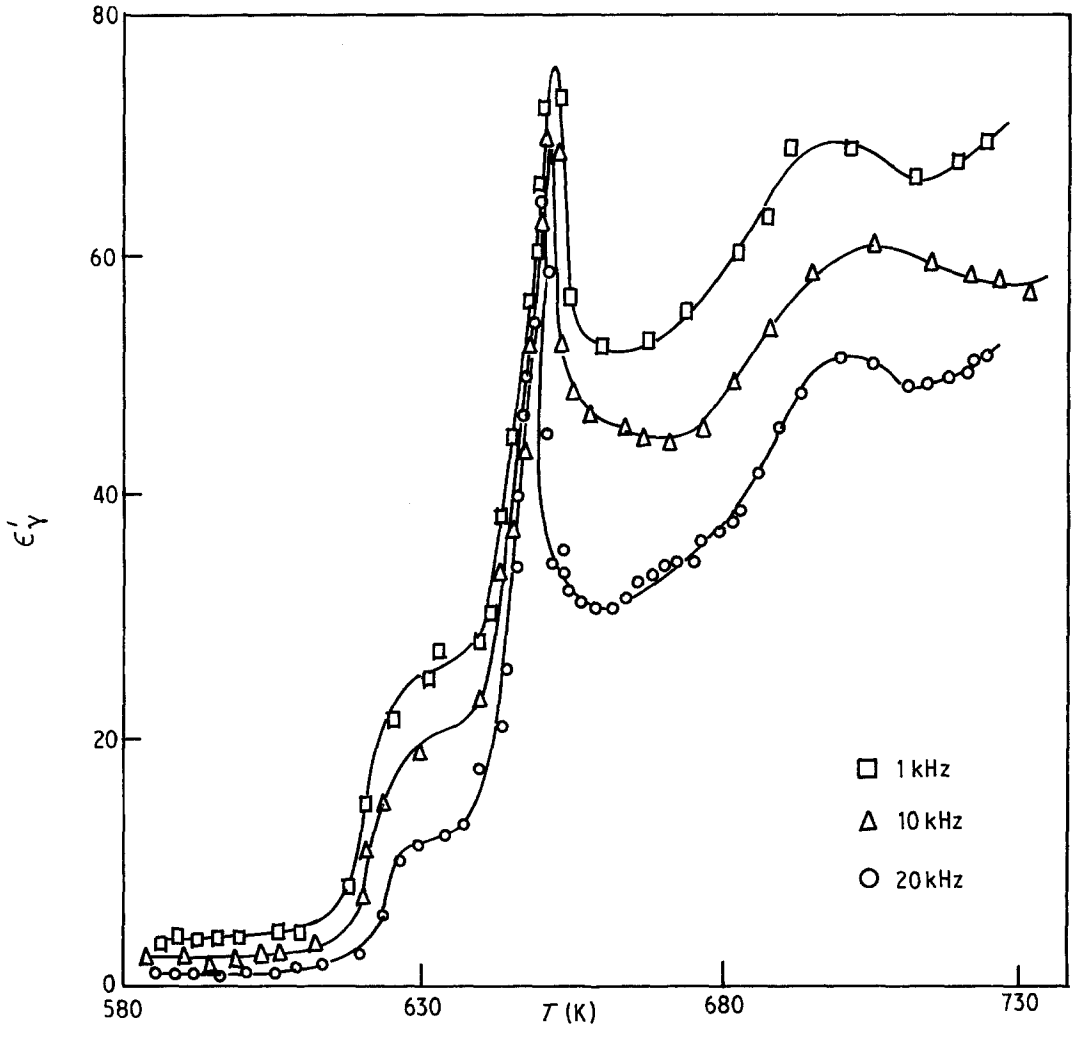

Figure 5 Variation of dielectric constant of $Nd(IO_3)_3$ with temperature.

of progressive filling of electrons in the deep-seated f-orbitals. Several systematics [23–26] have been proposed to rationalize small variation in properties observed thoughout the series. In the series cerium to europium, the ΔH values for type V → type IV and type IV → type I transformations increase monotonically with the increase in atomic number of the element. The ΔH values for gadolinium and terbium iodates which correspond to amorphous → type I conversion are quite high (*c.* 2.4 kcal mol^{-1}) (1 cal = 1.48 J) relative to that observed in the cerium to samarium series (*c.* 0.4 kcal mol^{-1}). In the series dysprosium to lutetium, the first endothermic effect (amorphous → amorphous) is very weak but the exothermic effect due to amorphous → type I transformation is very strong (~ 10 kcal mol^{-1}). The high ΔH value indicates that in this series the amorphous form is in a highly disordered state and therefore liberates a large amount of energy during crystallization. It may be noted that for all rare earth iodates excepting $La(IO_3)_3$, the type I phase is the highest temperature form. Crystal structure determination has been made for this phase with the archetype $Gd(IO_3)_3$ [5]. The reason why type VI is the highest temperature form for $La(IO_3)_3$ is not clear.

3.4. Dielectric properties of anhydrous iodates

The dielectric behaviour of $La(IO_3)_3$ has been reported previously [16]. Two maxima in ϵ_r against T at 370 and 510° C were observed. As found with DSC measurements, the dielectric properties of cerium, praseodymium, neodymium and samarium europium iodates are quite similar. Fig. 5 shows the variation in the dielectric constant of $Nd(IO_3)_3$ as a function of temperature

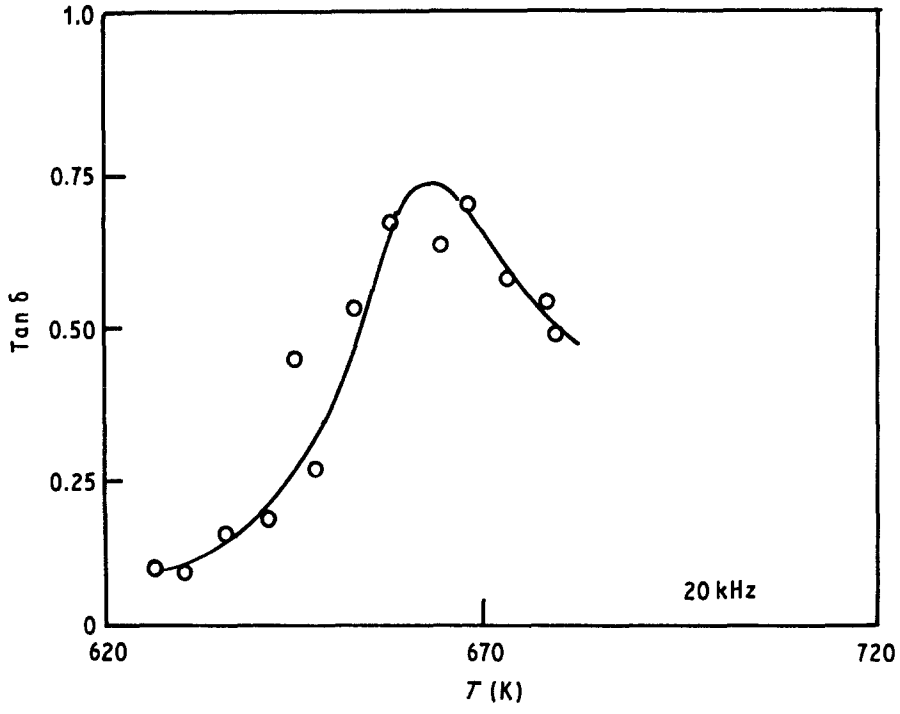

Figure 6 Variation of dielectric constant (above) and dielectric loss (overleaf) of $Gd(IO_3)_3$ with temperature.

at three different frequencies, namely 1, 10 and 20 kHz. At 20 kHz dielectric saturation occurs. The temperatures at which the inflections in ϵ_r against T occur are in good agreement with the transition temperatures obtained from DSC measurements. In Fig. 6 the variation in ϵ_r and loss tangent (tan δ) as a function of temperature and frequency are shown. In both cases a single inflection could be noted. Fig. 7 for $Dy(IO_3)_3$ typifies the dielectric behaviour of the compounds when Ln = dysprosium to lutetium. Here also a single peak in the ϵ_r against T plot is observed.

TABLE III Phase transition temperature (T_m) and dielectric constants (ϵ_r) obtained from dielectric measurements

$Ln(IO_3)_3$	T_m(° C)	Nature of transition	ϵ_r		
			1 kHz	10 kHz	20 kHz
La	369	Am → IV	30		22
	507	IV → I	66		57
Pr	364	Am → V	24	17	9
	377	V → IV	79	73	51
	417	IV → I	72	59	47
Nd	355	Am → V	25	19	12
		V → IV	76	71	65
		IV → I	70	60	52
Sm	357	Am → V			5
	391	V → IV			19
	451	IV → I			44
Gd	392	Am → I	49	42	35
Dy	403	Am → I	93		85
Tm	406	Am → I	97		88
Lu	398	Am → I	89		82

The results obtained with dielectric measurements are set out in Table III. The features observed for $Ln(IO_3)_3$ in DSC and dielectric measurements are in good agreement. However, the transition temperature (T_m) obtained in these two methods show some variation. This variation is mainly due to the difference in rates of heating and partly due to the difference in the techniques of temperature measurement. It may be noted that the dielectric constants for all the high temperature phases of $Ln(IO_3)_3$ are rather low, which probably indicates that all of them have centrosymmetric structures.

3.5. Dielectric properties of noncentrosymmetric hydrates

We have already reported [18] the low-temperature dielectric behaviour of $La(IO_3)_3 \cdot 0.5H_2O$ which is orthorhombic and has a space group, $P2_12_12_1$ [3]. The most interesting feature of this compound is that it has a high dielectric constant (ϵ_r, $c.2700$) at the ambient temperature and undergoes a phase transition between -130 to -150° C where the dielectric constant reaches a maximum (ϵ_r, $c.4200$).

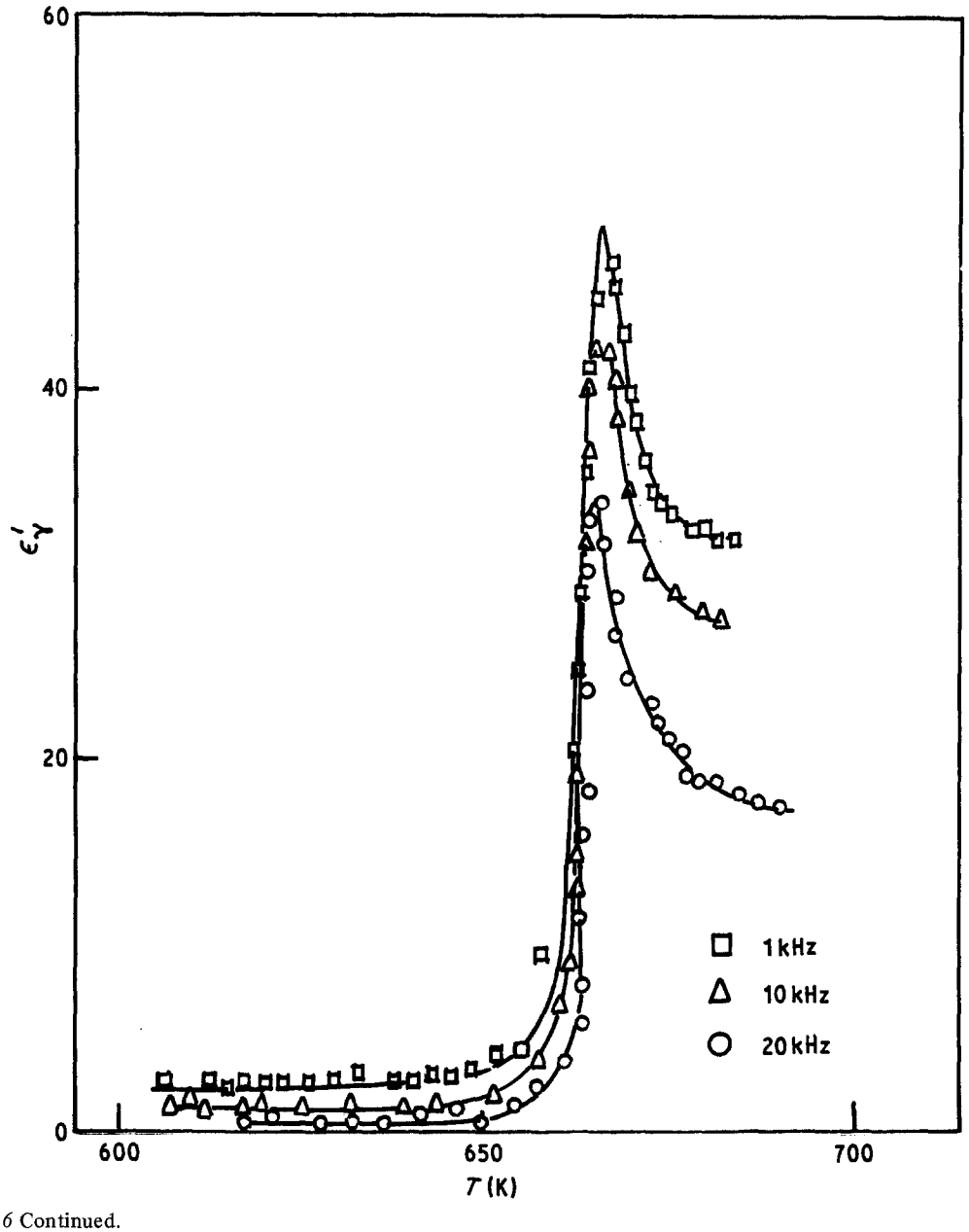

Figure 6 Continued.

We have recently investigated the compounds $Ln(IO_3)_3 \cdot H_2O$ (Ln = cerium, praseodymium, neodymium, samarium). All of them are monoclinic and have a space group $P2_1$ [3]. X-ray crystal structure [5], and piezoelectric (d_{22}) and pyroelectric (P_2) coefficients [7] for $Nd(IO_3)_3 \cdot H_2O$ have been determined. The dielectric properties of these compounds were investigated at 50 kHz in the temperature range 30 to $-160°$ C. All of these compounds have fairly high dielectric constants at ambient temperature and show little variation with temperature. For example, the value for ϵ_r measured at 50 kHz, lies in the range 2400 to 2000 for praseodymium, 1800 to 1500 for cerium, 1700 to 1400 for neodymium, and 1800 to 1400 for samarium in the entire range of study.

It may be pointed out that although application of dielectric analysis for thermophysical characterization of solids is well documented [27, 28], this technique is more useful for characterizing polymers rather than inorganic materials for which a technique like DTA is more commonly employed. Here we have shown that the two techniques are complementary to each other and if applied

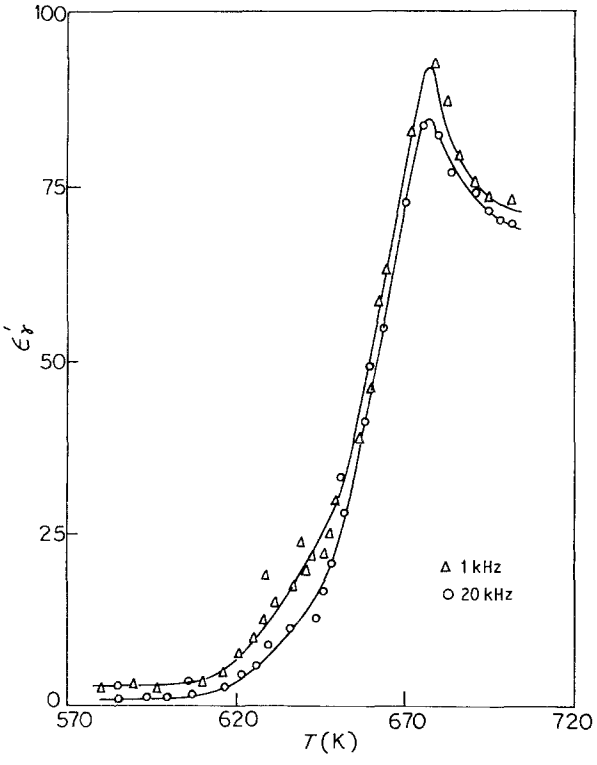

Figure 7 Variation of dielectric constant of $Dy(IO_3)_3$ with temperature.

together more insight can be obtained into the structure property relations in these materials.

Acknowledgements

This work was supported by the Council of Scientific and Industrial Research, India. We are grateful to Dr A. K. Ray for designing the dielectric cell.

References

1. K. NASSAU, J. W. SHIEVER, B. E. PRESCOTT and A. S. COOPER, *J. Solid State Chem.* **11** (1974) 314.
2. K. NASSAU, J. W. SHIEVER and B. E. PRESCOTT, *ibid.* **14** (1975) 122.
3. S. C. ABRAHAMS, J. L. BERNSTEIN and K. NASSAU, *ibid.* **16** (1976) 173.
4. *Idem, ibid.* **22** (1977) 243.
5. R. LIMINGA, S. C. ABRAHAMS and J. L. BERNSTEIN, *J. Chem. Phys.* **62** (1975) 755.
6. *Idem, ibid.* **67** (1977) 1015.
7. R. LIMINGA and S. C. ABRAHAMS, *J. Appl. Cryst.* **9** (1976) 42.
8. S. C. ABRAHAMS, J. L. BERNSTEIN, J. W. SHIEVER and K. NASSAU, *ibid.* **9** (1976) 357.
9. J. G. BERGMAN, G. D. BOYD, A. ASHKIN and S. KURTZ, *J. Appl. Phys.* **40** (1969) 2860.
10. E. T. KEVE, S. C. ABRAHAMS and J. L. BERNSTEIN, *J. Chem. Phys.* **54** (1971) 2556.
11. S. C. ABRAHAMS, R. C. SHERWOOD, J. L. BERNSTEIN and K. NASSAU, *J. Solid State Chem.* **7** (1973) 205.
12. G. M. YAKUNINA, L. A. ALEKSEENKO and V. V. SEREBRENNIKOV, *Russ. J. Inorg. Chem.* **14** (1969) 1414.
13. M. HARMELIN, *Compt. Rend.* **B262** (1966) 620.
14. B. HAJEK and J. HARDILOVA, *J. Less-Common Met.* **23** (1971) 217.
15. A. RAY, B. P. GHOSH and K. NAG, *Thermochim. Acta* **47** (1981) 105.
16. B. P. GHOSH, A. RAY and K. NAG, *J. Mater. Sci. Lett.* **2** (1983) 638.
17. J. L. McNAUGHTON and C. T. MORTIMER, "IRS; Physical Chemistry Series", Vol. 10 (Butterworths, London, 1975).
18. B. P. GHOSH, M. CHAUDHURY and K. NAG, *J. Solid State Chem.* **47** (1983) 307.
19. H. H. HOROWITZ and G. M. METZGER, *Anal. Chem.* **35** (1963) 1454.
20. A. W. COATS and J. P. REDFERN, *Nature* **201** (1964) 68.
21. G. G. SANYAL and K. NAG, *J. Inorg. Nucl. Chem.* **39** (1977) 1127.
22. A. K. RAY, M. CHAUDHURY and K. NAG, *Bull. Chem. Soc. Jpn.* **51** (1978) 1243.
23. D. F. PEPPARD, C. A. A. BLOOMQUIST, E. P. HORONITZ, S. LENEY and G. N. MASON, *J. Inorg. Nucl. Chem.* **32** (1970) 339.
24. I. FIDELIS and S. SIEKIERSKI, *ibid.* **33** (1971) 3191.

25. A. ROY and K. NAG, *ibid.* **40** (1978) 331.
26. S. P. SINHA, "Systematics and Properties of the Lanthanides" (Riedel, Dordrecht, 1983).
27. P. HEVDIG, "Dielectric Spectroscopy of Polymers" (Wiley, New York, 1977).
28. R. NOTTENBURG, K. RAJESHWAR, M. FREEMAN and J. DUBOW, *J. Solid State Chem.* **28** (1979) 195.

Received 30 April
and accepted 18 June 1984